

FASTLRNR AND SPARSE PHYSICS INFORMED BACKPROPAGATION

WOOJIN CHO*, KOOKJIN LEE†, NOSEONG PARK‡,
DONSUB RIM§, AND GERRIT WELPER¶

Abstract. We introduce *Sparse Physics Informed Backpropagation* (SPInProp), a new class of methods for accelerating backpropagation for a specialized neural network architecture called Low Rank Neural Representation (LRNR). The approach exploits the low rank structure within LRNR and constructs a reduced neural network approximation that is much smaller in size. We call the smaller network FastLRNR. We show that backpropagation of FastLRNR can be substituted for that of LRNR, enabling a significant reduction in complexity. We apply SPInProp to a physics informed neural networks framework and demonstrate how the solution of parametrized partial differential equations is accelerated.

Key words. low rank neural representation, neural networks, backpropagation, dimensionality reduction, physics informed machine learning, scientific machine learning

AMS subject classifications. 68T07, 65D25, 65M22

1. Introduction. Backpropagation is a key concept used in training deep learning models [12]. This paper concerns a technique for accelerating backpropagation via dimensionality reduction in a specialized neural network (NN) architecture called Low Rank Neural Representation (LRNR) [5, 21]. LRNRs have a built-in low rank factorization structure that grants them advantages in solving parametrized partial differential equations (pPDEs) [5], in particular for problems that proved challenging for physics informed neural networks (PINNs) [20, 17]. Theoretically, LRNRs are able to approximate complicated nonlinear shock interactions while maintaining low dimensionality and regular dynamics [21].

We show that, thanks to the LRNRs' low rank structure, smaller NN approximations we call FastLRNRs can be constructed. Backpropagation can be performed on the FastLRNR efficiently, and the resulting derivatives can be used to approximate derivatives of the original LRNR. Here we focus on presenting the main ideas and computationally study the simplest possible version. We anticipate many variants exploiting the same structure, and we refer to this class of methods accelerating backpropagation as *Sparse Physics Informed Backpropagation* (SPInProp). Here we focus on an accelerated solution of pPDEs, but SPInProp can potentially accelerate various computational tasks in deep learning models.

*Telepix, Seoul, 07330, South Korea (woojin@telepix.net)

†Department of Computer Science, Arizona State University, Phoenix, AZ 85281, USA (kookjin.lee@asu.edu)

‡School of Computing, Korea Advanced Institute of Science and Technology, Daejeon, 34141, South Korea (noseong@kaist.ac.kr)

§Department of Mathematics, Washington University in St. Louis, St. Louis, MO 63130, USA (rim@wustl.edu)

¶Department of Mathematics, University of Central Florida, Orlando, FL 32816, USA (gerrit.welper@ucf.edu)

2. General approach to SPInProp. In this section, we set up key definitions and put forth the main approach. We first define the LRNR architecture in Section 2.1, and present the associated FastLRNR architecture in Section 2.2.

2.1. Low Rank Neural Representation (LRNR). Given $n \in \mathbb{N}$, denote $[n] := \{1, \dots, n\}$ and $[n]_0 = [n] \cup \{0\}$. A *feedforward NN* for given depth $L \in \mathbb{N}$ and widths $(M_0, \dots, M_L) \in \mathbb{N}^{L+1}$ is a function $f : \mathbb{R}^{M_0} \rightarrow \mathbb{R}^{M_L}$ defined as the sequence of compositions

$$(2.1) \quad z^\ell = \sigma(W^\ell z^{\ell-1} + b^\ell), \quad \ell \in [L-1], \quad z^L = W^L z^{L-1} + b^L,$$

where the weight matrices $W^\ell \in \mathbb{R}^{M_\ell \times M_{\ell-1}}$ and bias vectors $b^\ell \in \mathbb{R}^{M_\ell}$ for $\ell \in [L]$ are called the parameters of the NN, and the nonlinear activation function $\sigma : \mathbb{R} \rightarrow \mathbb{R}$ acts entrywise. The input to the NN is $z^0 \in \mathbb{R}^{M_0}$ and the output is $z^L \in \mathbb{R}^{M_L}$. We denote the maximum width by $M_{\max} := \max_{\ell \in [L]_0} M_\ell$, the total width by $M_{\text{total}} := \sum_{\ell \in [L]_0} M_\ell$, the collection of the weights and biases $W := (W^\ell)_{\ell \in [L]}$ and $b := (b^\ell)_{\ell \in [L]}$, respectively.

Implicit Neural Representation (INR) is a dense NN whose input dimension M_0 is the spatio-temporal dimension and its output dimension M_L is the vector dimension of physical variables (density, temperature, pressure, etc). So the dimensions M_0 and M_L are relatively small. For example, an INR representing a solution to a scalar PDE in \mathbb{R}^2 has $M_0 = 2$ and $M_L = 1$.

To define LRNRs, we start by defining an INR $u_{\text{INR}} : \mathbb{R}^{M_0} \rightarrow \mathbb{R}^{M_L}$ whose weight matrix W^ℓ is substituted by the product of three weight matrices

$$(2.2) \quad W^\ell = U^\ell S^\ell V^{\ell\top}, \quad \ell \in [L],$$

with the individual factors taking on the form $U^\ell := [U_1^\ell \mid \dots \mid U_{r_\ell}^\ell] \in \mathbb{R}^{M_\ell \times r_\ell}$, $V^\ell := [V_1^\ell \mid \dots \mid V_{r_\ell}^\ell] \in \mathbb{R}^{M_\ell \times r_\ell}$, $S^\ell := \text{diag}(s^\ell) \in \mathbb{R}^{r_\ell \times r_\ell}$. We denote $s^\ell = (s_1^\ell, \dots, s_{r_\ell}^\ell) \in \mathbb{R}^{r_\ell}$ and assume all entries in s^ℓ to be non-negative. We let $r := (r_\ell)_{\ell \in [L]}$, $r_{\max} := \max_{\ell \in [L]} r_\ell$, $r_{\min} := \min_{\ell \in [L]} r_\ell$ and $r_{\text{total}} := \sum_{\ell \in [L]} r_\ell$.

The factored re-formulation (2.2) of the weight matrices (2.1) resembles the singular value decomposition (SVD) in its appearance [11], and if we assume $r_\ell \ll M_\ell$ for all $\ell \in [L]$ the products (2.2) form low rank matrices. Note that the same treatment is possible for the bias terms b^ℓ , but we will not factor the bias here (however, see [21] where the bias is similarly factored and plays a central role).

We collect these matrices with the notations $U := (U^\ell)_{\ell \in [L]}$, $V := (V^\ell)_{\ell \in [L]}$, and $s := (s^\ell)_{\ell \in [L]}$. We refer specifically to parameters in s as *coefficient parameters*, and to the parameters in (U, V) as *bases parameters*; they will play distinct roles. Note that s has $\mathcal{O}(Lr_{\max})$ parameters, whereas U and V each have $\Omega(M_{\max}r_{\min})$ parameters. The quadruple (U, V, b, s) contains all the parameters of u_{INR} so one can express its full parametric dependence by writing

$$(2.3) \quad u_{\text{INR}}(\cdot) = u_{\text{INR}}(\cdot; U, V, b, s).$$

The meta-learning framework proposed in [5] has two different phases for training the parameters (U, V, b, s) . In the *first phase*, or the *meta-learning phase*, the

bases parameters and the biases (U, V, b) are learned. Once learned, they are fixed as (U_*, V_*, b_*) , leaving us with a family of INRs

$$(2.4) \quad u_{\text{LRNR}}(\cdot; s) := u_{\text{INR}}(\cdot; U_*, V_*, b_*, s), \quad s \in \mathbb{R}^{r_{\text{total}}}.$$

If we suppose $r_\ell \ll M_{\text{max}}$ then we have $r_{\text{total}} \ll M_{\text{total}}$, and u_{LRNR} depends now solely on a small number of coefficient parameters in s , although it can generally have large widths. We refer to this low-dimensional family of INRs as a *Low Rank Neural Representation* (LRNR). Upon the completion of the meta-learning phase only the coefficient parameters s are assumed to be trainable, and they are trained during the *second phase*, or the *fine-tuning phase*. We defer further details to Section 3.

We now discuss the meta-learning framework in the context of solving pPDEs. Many scientific computing problems are naturally posed as pPDE problems [15], and in a pPDE, there is a vector of relevant physical parameters μ lying in a domain $\mathcal{D} \subset \mathbb{R}^p$ ($p \in \mathbb{N}$). The goals of the two phases are, respectively: (1) Find a LRNR with trained bases and biases tailored to the pPDE; (2) For queried μ , determine the coefficient parameters $s(\mu)$ that yields the approximation of the pPDE solution $u(\cdot; \mu)$ in the LRNR form

$$(2.5) \quad u(\cdot; \mu) \approx u_{\text{LRNR}}(\cdot; s(\mu)) = u_{\text{INR}}(\cdot; U_*, V_*, b_*, s(\mu)).$$

The relationship $s(\mu)$ is learned by backpropagation-based approaches, using u_{LRNR} as an ansatz in the pPDE. This meta-learning framework was named the Low Rank PINNs (LR-PINNs¹) in [5].

2.2. FastLRNRs. We turn our attention to the dimensionality reduction of LRNRs. The key idea is to construct an approximation to the s -independent parts of u_{LRNR} (2.4). Taking two contiguous layers, we write the part between the coefficient parameters s^ℓ 's as $\rho^\ell(\cdot) := V^{(\ell+1)\top} \sigma(U^\ell \cdot)$ and view it as a projected version of the nonlinear activation σ (we omit the biases for ease of exposition). It is known that when a scalar nonlinear function is applied to low rank vectors, the function values themselves can be well-approximated by low rank bases in certain situations [7, 2, 4, 3, 15]. A family of well-known and simple techniques can be applied to obtain an approximation to ρ^ℓ of the form

$$(2.6) \quad \zeta^\ell(\cdot) := \hat{V}^{(\ell+1)\top} \sigma(\hat{U}^\ell \cdot), \quad \ell \in [L-1],$$

in which the reduced bases parameters now have the dimensions $\hat{U}^\ell \in \mathbb{R}^{\hat{r}_\ell \times r_\ell}$ and $\hat{V}^{\ell+1} \in \mathbb{R}^{\hat{r}_{\ell+1} \times r_{\ell+1}}$, and the reduced dimensions are small in the sense $\hat{r}_\ell \sim r_\ell \ll M_{\text{max}}$. We write $\hat{r} := (\hat{r}_\ell)_{\ell \in [L-1]}$ and $\hat{r}_{\text{max}} := \max_{\ell \in [L-1]} \hat{r}_\ell$.

For example, consider the use of the empirical interpolation method (EIM/DEIM [2, 4]). Writing out the EIM approximation, which uses a subsampling of the state vectors, we have

$$(2.7) \quad \rho^\ell(\cdot) \approx \zeta_{\text{EIM}}^\ell(\cdot) := V^{(\ell+1)\top} \Xi^\ell (P^{\ell\top} \Xi^\ell)^{-1} \sigma(P^{\ell\top} U^\ell \cdot), \quad \Xi^\ell \in \mathbb{R}^{M_\ell \times \hat{r}_\ell}, \quad \hat{r}_\ell \in \mathbb{N},$$

¹LRNR refers specifically to the architecture, and LR-PINNs to the overarching meta-learning framework using LRNRs.

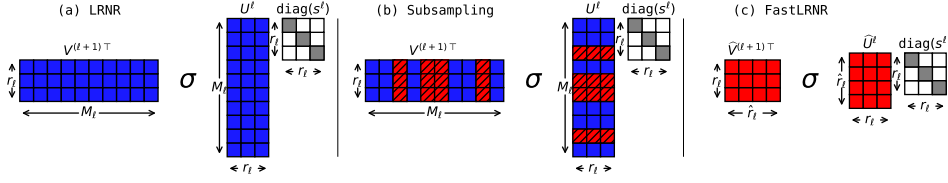


Fig. 2.1: An illustration of the (a) LRNR and the associated (c) FastLRNR architectures, obtained by e.g. subsampling the rows of the low rank matrices as shown in (b).

where $P^\ell \in \mathbb{R}^{M_\ell \times \hat{r}_\ell}$ is a sampling matrix made up of subcolumns of a $M_\ell \times M_\ell$ identity matrix, and $\Xi^\ell \in \mathbb{R}^{M_\ell \times \hat{r}_\ell}$ is a matrix with linearly independent columns whose square subblock $P^{\ell\top} \Xi^\ell \in \mathbb{R}^{\hat{r}_\ell \times \hat{r}_\ell}$ is invertible. Viewed in the general form (2.6), this approximation has $\hat{U}^\ell = P^{\ell\top} U^\ell$ and $\hat{V}^{\ell+1} = V^{(\ell+1)\top} \Xi^\ell (P^{\ell\top} \Xi^\ell)^{-1}$.

Inserting (2.6) into the LRNR architecture, one obtains $\hat{z}^\ell = \zeta^\ell(\text{diag}(s^\ell) \hat{z}^{\ell-1})$ where the multiplication by $\text{diag}(s^\ell)$ can be rewritten using the notation \odot for the Hadamard (elementwise) product. Concisely,

$$(2.8) \quad \hat{z}^\ell = \zeta^\ell(s^\ell \odot \hat{z}^{\ell-1}), \quad \ell \in [L-1], \quad \hat{z}^L = U^L(s^L \odot \hat{z}^{L-1}).$$

Then we have an approximation of the hidden states z^ℓ in the original LRNR (2.1) purely in terms of the approximate projected/reduced states, that is

$$\hat{z}^\ell \approx V^{(\ell+1)\top} z^\ell, \quad \ell \in [L-1]_0, \quad \hat{z}^L \approx z^L.$$

Note that in the input and output layers, the reduction can be trivial.

We refer to the reduced form of LRNR (2.8), as a *FastLRNR* $\hat{u}_{\text{FAST}}: \mathbb{R}^{M_0} \rightarrow \mathbb{R}^{M_L}$. Diagrams in Figure 2.1 compare the LRNR versus the FastLRNR architectures, and illustrate the subsampling strategy devised in EIM in this context. We remark that the approximation still has the structure of NNs (2.1), except that the nonlinear activation functions σ correspond to specialized functions ζ^ℓ , which are generally different functions depending on the layer (cf. [18]). In this analogy, the Hadamard products with s^ℓ in (2.8) play the role of affine mappings in (2.1), and in this sense FastLRNRs (2.8) (and LRNRs) are said to be *diagonalizable*.

2.3. SPInProp via backpropagation of FastLRNR. SPInProp complexity depends only on L and the small dimension r_{\max} . Comparing the backpropagation complexities: (1) For NNs (2.1) with parameters (W, b) , $\mathcal{O}(LM_{\max}^2)$ operations; (2) For LRNR u_{LRNR} (2.4) with parameters s , $\mathcal{O}(LM_{\max} r_{\max})$; (3) For FastLRNR \hat{u}_{FAST} (2.8) with parameters s , $\mathcal{O}(Lr_{\max}^2)$.

3. Fast Low Rank PINNs (Fast-LR-PINNs). We seek to demonstrate that SPInProp operations can be used to efficiently perform backpropagation operations when solving pPDEs. To this end, we devise computational experiments in the LR-PINNs meta-learning framework [5] with important additions. We discuss the meta-learning phase in Section 3.1. A new phase using SPInProp, which we call the *fast phase*, is introduced in Section 3.2

3.1. Meta-Learning with Sparsity Promoting Regularization. As discussed in Section 2.1, during the meta-learning phase the bases and bias parameters (U, V, b) are trained. This is done using a hypernetwork representation of $s(\mu)$ (see (2.5)). We define a hypernetwork $f_{\text{hyper}} : \mathcal{D} \rightarrow \mathbb{R}_+^{r_{\text{total}}}$ which is itself a NN (2.1) whose widths satisfy $M_{\text{hyper}, \ell} \sim r_{\text{total}}$ and has an extra ReLU applied so that the outputs are non-negative. We call its NN parameters Θ and write $f(\cdot) = f(\cdot; \Theta)$.

The meta-network is used during this phase, defined as

$$(3.1) \quad u_{\text{META}}(\cdot; \mu, U, V, b, \Theta) := u_{\text{INR}}(\cdot; U, V, b, f_{\text{hyper}}(\mu; \Theta)).$$

This model results from a type of output-to-parameter concatenation between (a) u_{INR} with low rank structure in its parameters (2.3), and (b) f_{hyper} whose non-negative outputs feed into u_{INR} as coefficients s .

The PINNs loss for the meta-learning phase is given by

$$(3.2) \quad \begin{aligned} \mathcal{L}_{\text{meta}}(U, V, b, \Theta) := & \mathbb{E}_{(\cdot, \mu)} \left[|\mathcal{N}[u_{\text{META}}; \mu](\cdot; \mu, U, V, b, \Theta)|^2 \right] \\ & + \mathbb{E}_{(\cdot, \mu)} \left[|\mathcal{B}[u_{\text{META}}; \mu](\cdot; \mu, U, V, b, \Theta)|^2 \right] \end{aligned}$$

where $\mathcal{N}[\cdot; \mu]$ denotes a (nonlinear) differential operator, and $\mathcal{B}[\cdot; \mu]$ the initial-boundary operator. The expectation is taken over some probability measure over the PDE domain Ω and physical parameter domain \mathcal{D} as specified in the pPDE problem. Uniform measure is commonly used.

We define the orthogonality regularization term and the sparsity-promoting regularization term as

$$(3.3) \quad \begin{aligned} \mathcal{R}_{\text{orth}}(U, V) := & \sum_{\ell \in [L]} \|U^{\ell \top} U^\ell - I^\ell\|_F^2 + \|V^{\ell \top} V^\ell - I^\ell\|_F^2, \\ \mathcal{R}_{\text{sparse}}(\Theta) := & \mathbb{E}_\mu \left[\sum_{\ell \in [L]} \|\sigma(\Gamma^\ell f_{\text{hyper}}^\ell(\mu; \Theta))\|_1 \right], \end{aligned}$$

where $I^\ell \in \mathbb{R}^{r_\ell \times r_\ell}$ are identity matrices, $\|\cdot\|_F$ denotes the Frobenius norm, and where the matrices $\Gamma^\ell \in \mathbb{R}^{(r_\ell - 1) \times r_\ell}$ are banded matrices with -1's on the diagonal and γ on the 1st super-diagonal ($\gamma \geq 1$ is a hyperparameter). The motivation for adding $\mathcal{R}_{\text{sparse}}$ is to promote the sparsity in the coefficient parameters s in u_{INR} above (3.1), thereby constraining the meta-network u_{META} to become as low rank as possible. In u_{META} the coefficient parameters are coupled to the f_{hyper} output variables, so we enforce the sparsity on the parameters Θ of f_{hyper} . When $\mathcal{R}_{\text{sparse}}$ is zero the coefficient parameters s^ℓ (which are output from f_{hyper}^ℓ) satisfy $(1/\gamma)s_i^\ell > s_{i+1}^\ell$ so a geometric rate of decay is achieved. An apparently more intuitive [8] choice of taking the 1-norm $\|f_{\text{hyper}}^\ell(\mu; \Theta)\|_1$ was less successful in promoting sparsity in our experiments.

Finally, the meta-learning problem is given by

$$(3.4) \quad \min_{U, V, b, \Theta} \mathcal{L}_{\text{meta}}(U, V, b, \Theta) + \lambda_{\text{orth}} \mathcal{R}_{\text{orth}}(U, V) + \lambda_{\text{sparse}} \mathcal{R}_{\text{sparse}}(\Theta).$$

3.2. Fast phase. At the end of the meta-learning phase, we have learned the bases and bias parameters (U_*, V_*, b_*) , along with the hypernetwork parameters Θ_* .

This brings us to the fine-tuning phase, where one solves the PDE for any given physical parameter $\mu \in \mathcal{D}$ by fine-tuning the u_{LRNR} coefficient parameters s (2.4) as informed by the differential equations. The coefficients s are initialized at the hypernetwork prediction value $f_{\text{hyper}}(\mu; \Theta_*)$. During this phase, the learning problem is to minimize the physics-informed loss function over a small number of coefficient parameters s ,

$$(3.5) \quad \min_s \mathcal{L}_{\text{tune}}(s; \mu),$$

where $\mathcal{L}_{\text{tune}}(s; \mu) := \mathbb{E} \left[|\mathcal{N}[u_{\text{LRNR}}; \mu](\cdot; s)|^2 \right] + \mathbb{E} \left[|\mathcal{B}[u_{\text{LRNR}}; \mu](\cdot; s)|^2 \right]$.

In the previous experiments [5], the fine-tuning phase for u_{LRNR} was found to reliably yield improved PDE solutions. Now, if FastLRNR \hat{u}_{FAST} (2.8) is a type of an approximation of u_{LRNR} , it is natural to attempt to update the coefficient parameters s using the smaller \hat{u}_{FAST} , and test if these updates result in improved solutions. If they do, it means updates using \hat{u}_{FAST} alone can lead to improved coefficient values $s_{\text{fast}}(\mu)$, at the computationally cheaper cost of SPInProp operations (Section 2.3).

We newly introduce the fast phase during which we solve a learning problem for \hat{u}_{FAST} . Following a subsampling strategy (Section 2.2), we define a sparsely sampled version of the fine-tuning-phase loss $\mathcal{L}_{\text{tune}}$,

$$(3.6) \quad \mathcal{L}_{\text{fast}}(s; \mu) := \sum_{\cdot \in \mathcal{X} \cap \Omega} |\mathcal{N}[\hat{u}_{\text{FAST}}; \mu](\cdot; s)| + \sum_{\cdot \in \mathcal{X} \cap \partial\Omega} |\mathcal{B}[\hat{u}_{\text{FAST}}; \mu](\cdot; s)|,$$

where $\mathcal{X} \subset \Omega \cap \partial\Omega$ is a set of sparse sampling points. Here we have used the ℓ_1 error, motivated by the L_1 minimization formulation of convective problems [14, 13].

A naïve approach would be to substitute the higher-dimensional learning problem (3.5) by a lower-dimensional one, replacing the loss $\mathcal{L}_{\text{tune}}$ with a direct analogue $\mathcal{L}_{\text{fast}}$. However, this approach did not automatically lead to improvements in the solution in our experiments. While the training loss decreases consistently, the FastLRNR solution $u_{\text{LRNR}}(\cdot; s)$ eventually diverges away from the true solution despite improvement during the initial epochs. This suggests the naïve learning problem is affected by a type of generalization issue. We speculate there are two possible causes. First, FastLRNR performs sparse sampling of both the PDE domain and the hidden states, possibly incurring bias that leads to generalization errors. Second, FastLRNR performs projections at each layer and the effect of these projections on stability can be significant and complex, potentially causing this issue; related stability issues arise in simpler linear models like reduced basis methods (see e.g. [22, 9, 10, 6]).

To deal with the generalization issue, we regularize the naïve learning problem by adding a locality regularization term for the coefficient parameters s . We set the fast phase learning problem as

$$(3.7) \quad \min_s \mathcal{L}_{\text{fast}}(s; \mu) + \lambda_{\text{loc}} \mathcal{R}_{\text{loc}}(s; \mu), \quad \mathcal{R}_{\text{loc}}(s; \mu) := \sum_{\ell \in [L]} \|s^\ell - f_{\text{hyper}}^\ell(\mu)\|_1.$$

Once this optimization problem is solved, the solution $s_{\text{fast}}(\mu)$ can be used in the original LRNR representation. Note that the problem (3.7) was informed by physics at the sampling points \mathcal{X} , implying that \hat{u}_{FAST} is trained to be close to u_{LRNR} only

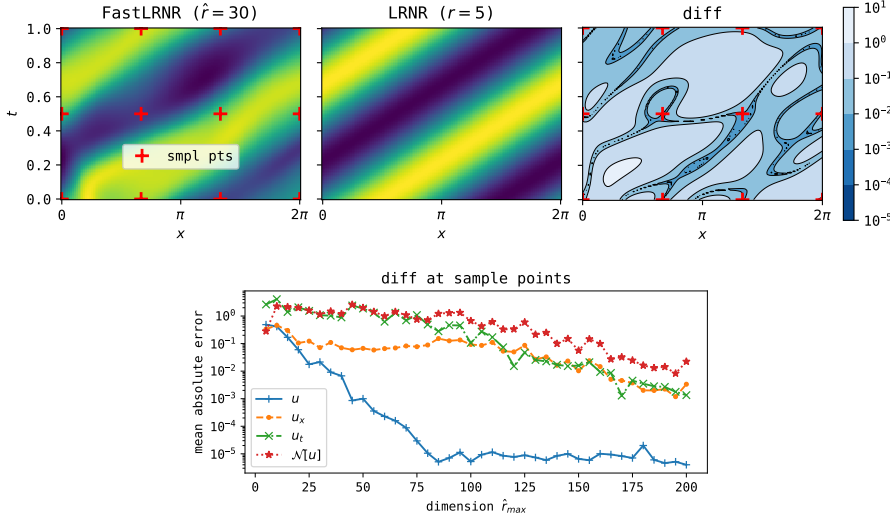


Fig. 3.1: The pointwise value difference between the FastLRNR \hat{u}_{FAST} and LRNR u_{LRNR} for the convective case $\mathcal{D}_{\text{conv}}$ 4.2 with physical parameter $\mu = (7, 0, 0)$ and dimension $\hat{r}_{\text{max}} = 30$. The sparse sampling points in \mathcal{X} are marked by $+$. The FastLRNR is a much smaller than LRNR but agrees with it at the sampling points (top). SPInProp accuracy versus discrete dimension \hat{r}_{max} ($\ell = 2, 3, 4$), mean absolute error over the uniform sampling points $\mathcal{X} \subset \Omega$ (bottom).

at these points. To obtain a solution that is accurate for the entire domain Ω , we make use of the original LRNR architecture, setting as the solution $u_{\text{FASTSOL}}(\cdot; \mu) := u_{\text{LRNR}}(\cdot; s_{\text{fast}}(\mu))$. In short, we return to the architecture with possibly large widths, once the coefficient parameters s are updated via gradient descent using only \hat{u}_{FAST} and SPInProps.

4. Parametrized convection-diffusion-reaction problem. We consider a parametrized initial boundary value problem: Convection-diffusion-reaction on the spatio-temporal domain $\Omega := (0, 2\pi) \times (0, 1)$ with periodic boundary conditions. We seek the solution $u : \Omega \rightarrow \mathbb{R}$ satisfying the following PDE with non-negative physical parameters $\mu = (\mu_1, \mu_2, \mu_3)$,

$$\begin{aligned}
 \mathcal{N}[u; \mu] &= 0, \quad (x, t) \in \Omega, \\
 \text{where } \mathcal{N}[u; \mu] &:= \partial_t u + \mu_1 \partial_x u - \mu_2 \partial_{xx} u - \mu_3 u(1 - u), \\
 u(x, 0) &= \sin(x), \quad x \in (0, 2\pi), \quad u(0, t) = u(2\pi, t), \quad t \in (0, 1).
 \end{aligned}
 \tag{4.1}$$

We consider two physical parameter domains: The first is a pure convection problem, and the second is the full convection-diffusion-reaction problem:

$$\mathcal{D}_{\text{conv}} = \text{diag}([\mu_{\text{conv}, \min}, \mu_{\text{conv}, \max}]), \quad \mathcal{D}_{\text{cdr}} = \text{diag}([\mu_{\text{cdr}, \min}, \mu_{\text{cdr}, \max}]),
 \tag{4.2}$$

where we set $\mu_{\text{conv}, \min} = (5, 0, 0)$, $\mu_{\text{conv}, \max} = (8, 0, 0)$, $\mu_{\text{cdr}, \min} = (1, 0, 0)$, $\mu_{\text{cdr}, \max} = (3, 2, 2)$. The PDE is nonlinear and is highly convective when the diffusion term μ_2

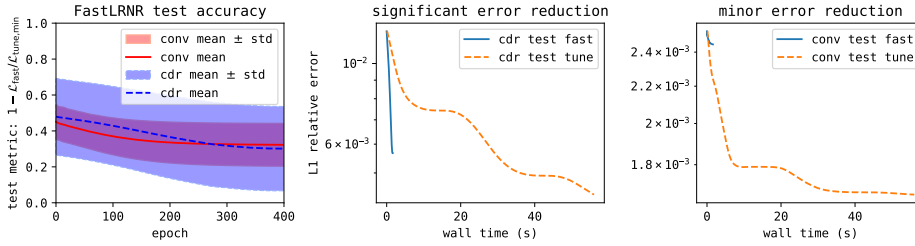


Fig. 4.1: Plots comparing the accuracy of FastLRNR and LRNR over 20 test cases. Comparing the FastLRNR test loss to the minimal test loss $\mathcal{L}_{\text{tune}}$ achieved with LRNR, FastLRNR cheaply obtains nearly half of the test loss accuracy of LRNR (left). To the right are shown two L^1 relative error plots versus wall time. In the majority (16 out of 20) of test examples, within one second of starting the optimization problem (3.7), FastLRNR achieves slightly worse L^1 relative error compared to LRNR (middle). In a minority of test examples (4 out of 20), only a minor error reduction is achieved, although in these cases errors were lower overall (right).

is small. This is a numerical example from [5] where the PDE was used in extreme regimes to test the effectiveness of the meta-learning approach.

Our PyTorch-based [19] implementation of FastLRNR is based on that of [5], and is available in a public code repository [1]. We refer the readers to the repository for the precise details that are omitted here.

Upon completing the meta-learning phase using a meta-network of size $M_{\text{max}} = 4000$ and $r_{\text{max}} = 100$, most of the predicted coefficient outputs from f_{hyper} are identically zero. These coefficients are dropped and the corresponding columns of bases parameters (U, V) are truncated. The coefficient dimensions of LRNRs are adjusted correspondingly, yielding $r = (1, 5, 5, 3, 1)$ for $\mathcal{D}_{\text{conv}}$ and $r = (1, 49, 30, 25, 1)$ for \mathcal{D}_{cdr} . This computation implies that LRNR solutions with $r_{\text{max}} \ll M_{\text{max}}$ exist for this pPDE for $\mathcal{D}_{\text{conv}}$ and \mathcal{D}_{cdr} .

Next, we construct the associated FastLRNR (2.8). We proceed by evaluating u_{LRNR} at fixed input sampling points \mathcal{X} and their perturbations, across various parameters values in \mathcal{D} . We choose 4-by-3 uniform grid points as the 12 input sampling points \mathcal{X} , then we use EIM to compute (Ξ^ℓ, P^ℓ) (2.7). Since \hat{u}_{FAST} and u_{LRNR} share the coefficient parameters, comparing them as spatio-temporal functions on Ω can be instructive. In Figure 3.1, \hat{u}_{FAST} with $\hat{r}_{\text{max}} = 30$ is compared with u_{LRNR} , with coefficients initialized as $f_{\text{hyper}}(\mu)$ and $\mu = (7, 0, 0)$ for both. We see that they (and their derivatives) agree at the sampling points.

Finally, the learning problems for the FastLRNR (3.7) and the LRNR (3.5) are solved using Adam [16] up to 400 epochs for 20 test examples (10 in $\mathcal{D}_{\text{conv}}$ and 10 in \mathcal{D}_{cdr}). The test accuracy of these solutions are shown in Figure 4.1. In most examples, FastLRNR achieves L^1 relative error close to that of LRNR for $\hat{r}_{\text{max}} = 5$, and this accuracy is achieved within a fraction of a second, owing to the computational speed of SPInProp operations (Section 2.3). In some examples, the FastLRNR does not improve in accuracy, however in these subcases we found that the initial guess for the

coefficients from f_{hyper} was already very accurate.

The FastLRNR is roughly $\times 36$ faster than fine-tuning-phase training (for $M_{\text{max}} = 4000$, $r_{\text{max}} = 49$, $\hat{r}_{\text{max}} = 5$). Wall time for a single Adam step using SPInProp is 0.004s versus 0.14s for standard backpropagation on an NVIDIA V100 GPU with 32GB memory. In principle the speedup would be greater for even larger widths, since the complexity scales linearly with respect to the widths. Moreover, the fast phase can run on the CPU due to its small memory requirements.

Acknowledgements. The authors acknowledge the Research Infrastructure Services (RIS) group at Washington University in St. Louis for providing computational resources and services needed to generate the research results delivered within this paper (URL ris.wustl.edu). K. Lee acknowledges support from the U.S. National Science Foundation under grant IIS 2338909.

REFERENCES

- [1] *Code Repository FastLRNR*, 2024, doi:10.5281/zenodo.13892195.
- [2] M. BARRAULT, Y. MADAY, N. C. NGUYEN, AND A. T. PATERA, *An ‘empirical interpolation’ method: application to efficient reduced-basis discretization of partial differential equations*, *Comptes Rendus Mathematique*, 339 (2004), pp. 667 – 672.
- [3] K. CARLBERG, C. FARHAT, J. CORTIAL, AND D. AMSALLEM, *The GNAT method for nonlinear model reduction: Effective implementation and application to computational fluid dynamics and turbulent flows*, *Journal of Computational Physics*, 242 (2013), pp. 623–647.
- [4] S. CHATURANTABUT AND D. C. SORENSEN, *Nonlinear Model Reduction via Discrete Empirical Interpolation*, *SIAM Journal on Scientific Computing*, 32 (2010), pp. 2737–2764.
- [5] W. CHO, K. LEE, D. RIM, AND N. PARK, *Hypernetwork-based Meta-Learning for Low-Rank Physics-Informed Neural Networks*, in *Advances in Neural Information Processing Systems*, vol. 36, Red Hook, NY, 2023, Curran Associates, Inc., pp. 11219–11231.
- [6] W. DAHMEN, C. PLESKEN, AND G. WELPER, *Double greedy algorithms: Reduced basis methods for transport dominated problems*, *ESAIM: Mathematical Modelling and Numerical Analysis*, 48 (2014), pp. 623–663.
- [7] R. EVERSON AND L. SIROVICH., *The Karhunen-Loeve procedure for gappy data*, *Journal of the Optical Society of America A*, 12 (1995), pp. 1657–1664.
- [8] S. FOUCART AND H. RAUHUT, *A Mathematical Introduction to Compressive Sensing*, Birkhäuser, 2013.
- [9] A.-L. GERNER AND K. VEROY, *Reduced basis a posteriori error bounds for the Stokes equations in parametrized domains: A penalty approach*, *Mathematical Models and Methods in Applied Sciences*, 21 (2011), pp. 2103–2134.
- [10] A.-L. GERNER AND K. VEROY, *Certified Reduced Basis Methods for Parametrized Saddle Point Problems*, *SIAM Journal on Scientific Computing*, 34 (2012), pp. A2812–A2836.
- [11] G. H. GOLUB AND C. F. VAN LOAN, *Matrix Computations (3rd Ed.)*, Johns Hopkins University Press, Baltimore, MD, USA, 1996.
- [12] I. GOODFELLOW, Y. BENGIO, AND A. COURVILLE, *Deep Learning*, MIT Press, Cambridge, MA, 2016. <http://www.deeplearningbook.org>.
- [13] J.-L. GUERMOND, F. MARPEAU, AND B. POPOV, *A fast algorithm for solving first-order PDEs by L1-minimization*, *Communications in Mathematical Sciences*, 6 (2008), pp. 199 – 216.
- [14] J.-L. GUERMOND AND B. POPOV, *Linear advection with ill-posed boundary conditions via l1-minimization*, *International Journal of Numerical Analysis and Modeling*, 4 (2007), pp. 39–47.
- [15] J. S. HESTHAVEN, G. ROZZA, AND B. STAMM, *Certified Reduced Basis Methods for Parametrized Partial Differential Equations*, Springer, Cham, 2016.
- [16] D. KINGMA AND J. BA, *Adam: A Method for Stochastic Optimization*, in *International Conference on Learning Representations (ICLR)*, San Diego, CA, USA, 2015.

- [17] A. KRISHNAPRIYAN, A. GHOLAMI, S. ZHE, R. KIRBY, AND M. W. MAHONEY, *Characterizing possible failure modes in physics-informed neural networks*, in Advances in Neural Information Processing Systems, vol. 34, Red Hook, NY, 2021, Curran Associates, Inc., pp. 26548–26560.
- [18] Z. LIU, Y. WANG, S. VAIDYA, F. RUEHLE, J. HALVERSON, M. SOLJAČIĆ, T. Y. HOU, AND M. TEGMARK, *KAN: Kolmogorov-Arnold Networks*, 2024, [arXiv:2404.19756](https://arxiv.org/abs/2404.19756).
- [19] A. PASZKE, S. GROSS, F. MASSA, A. LERER, J. BRADBURY, G. CHANAN, T. KILLEEN, Z. LIN, N. GIMELSHEIN, L. ANTIGA, A. DESMAISON, A. KOPF, E. YANG, Z. DEVITO, M. RAISON, A. TEJANI, S. CHILAMKURTHY, B. STEINER, L. FANG, J. BAI, AND S. CHINTALA, *Pytorch: An imperative style, high-performance deep learning library*, in Advances in Neural Information Processing Systems, vol. 32, 2019.
- [20] M. RAISSI, P. PERDIKARIS, AND G. KARNIADAKIS, *Physics-informed neural networks: A deep learning framework for solving forward and inverse problems involving nonlinear partial differential equations*, Journal of Computational Physics, 378 (2019), pp. 686–707.
- [21] D. RIM AND G. WELPER, *A Low Rank Neural Representation of Entropy Solutions*, (2024), [arXiv:2406.05694](https://arxiv.org/abs/2406.05694).
- [22] G. ROZZA AND K. VEROY, *On the stability of the reduced basis method for Stokes equations in parametrized domains*, Computer Methods in Applied Mechanics and Engineering, 196 (2007), pp. 1244–1260.